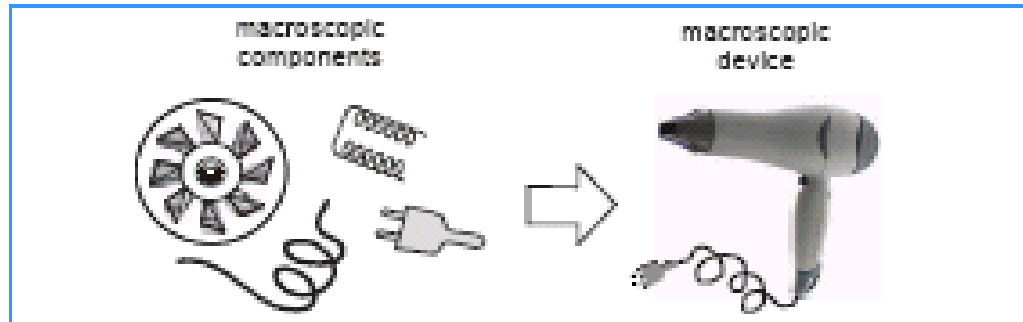
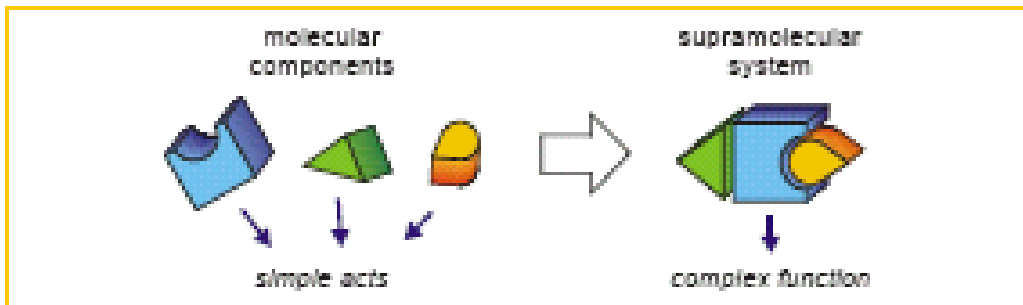


# Dispositivi e Macchine Molecolari

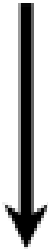
## Macroscopic device



## Molecular-level device



**design +  
synthesis**



**Molecular  
Components**



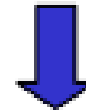
**self-assembly,  
self-organization**

*or*

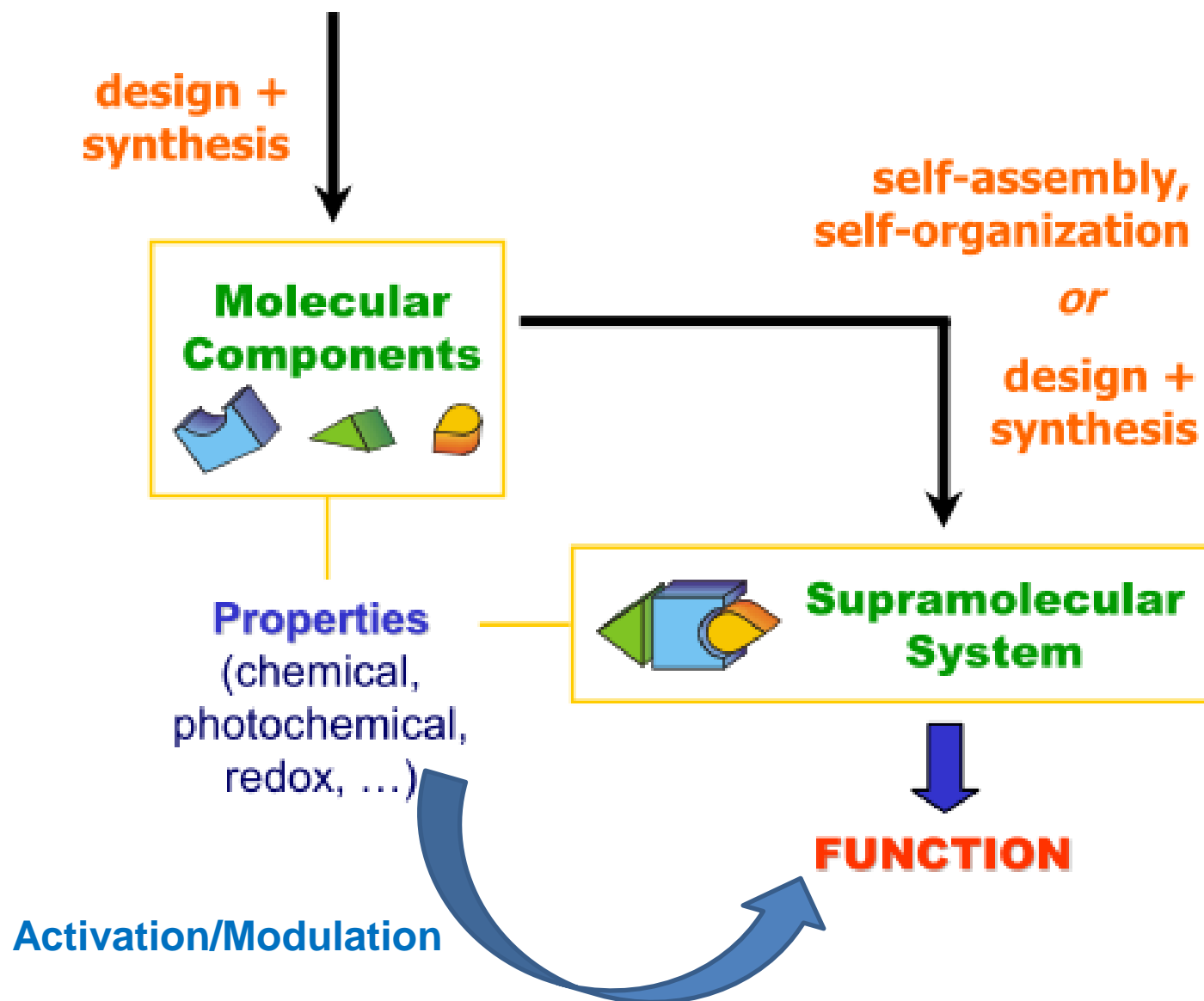
**design +  
synthesis**



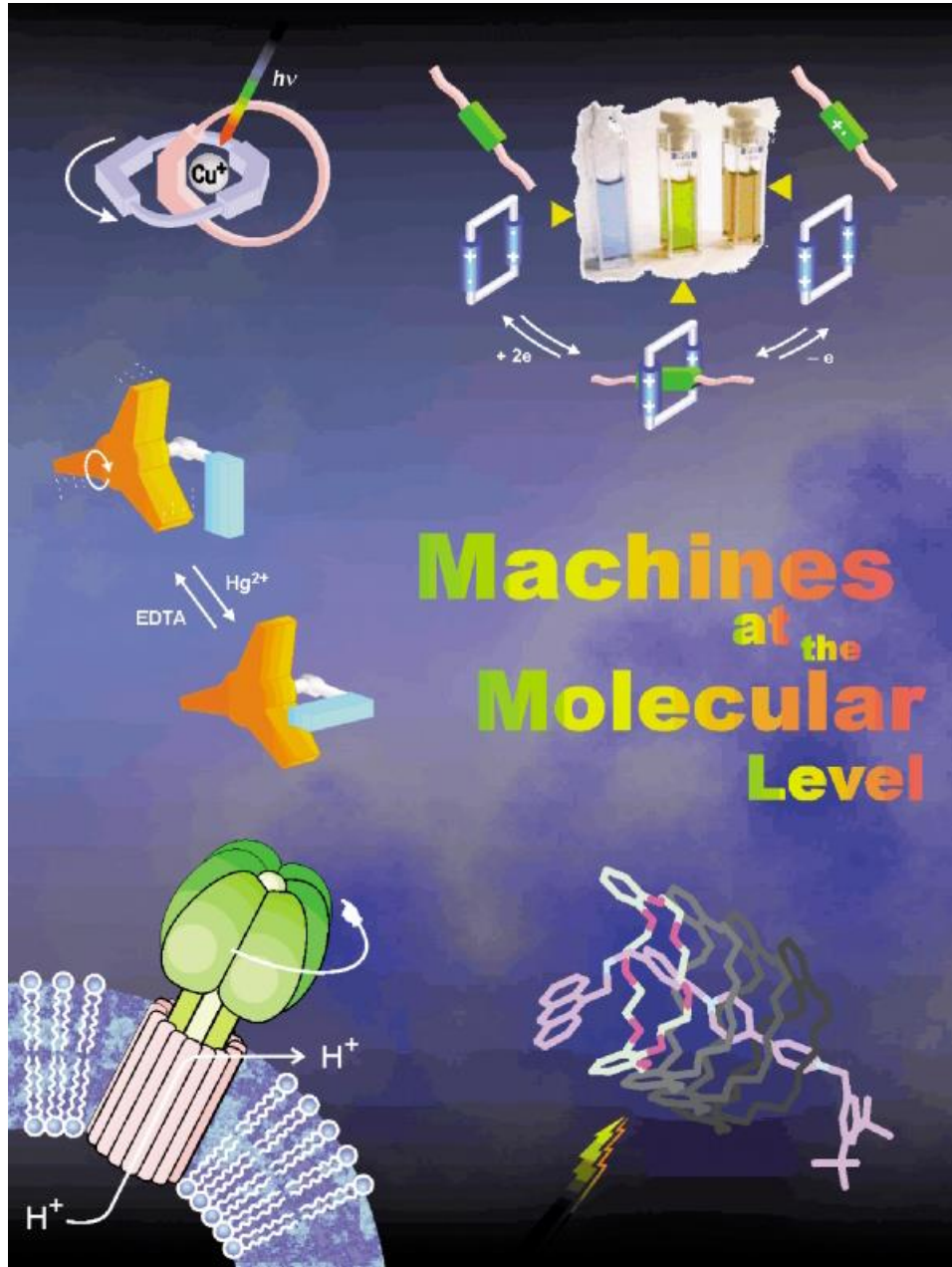
**Supramolecular  
System**



**FUNCTION**



- tipo di energia (chimica, fotoni, elettroni)
- monitoraggio (tecniche fotofisiche, elettrochimiche)
- processo ciclico
- tempo (picosecondi-minuti)
- funzione



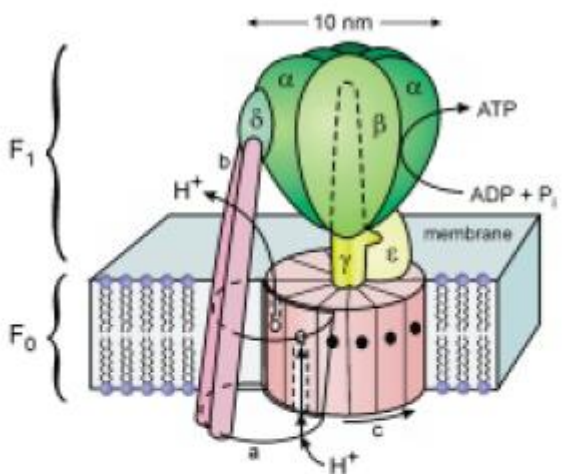


Figure 1. The structure of F<sub>0</sub>F<sub>1</sub>ATP synthase.<sup>[18]</sup> The catalytic region is composed of the subunits  $\alpha$ - $\epsilon$ . The proton channels lie at the interface between the subunits  $\alpha$  and  $c$  (dashed lines indicate the putative inlet and outlet channels). Proton flow through the channels develops torque between the  $\alpha$  and  $c$  subunits. This torque is transmitted to F<sub>1</sub> via the  $\gamma$  shaft and the  $\epsilon$  subunit, where it is used to release ATP sequentially from the catalytic sites in F<sub>1</sub>. The  $c$  subunit consists of 9–12 twin  $\alpha$ -helices arranged in a central membrane-spanning array. The  $\alpha$  subunit consists of 5–7 membrane-spanning  $\alpha$ -helices and is connected to F<sub>1</sub> by the  $b$  and  $\delta$  subunits. Reprinted by permission from ref. [16] (Copyright<sup>®</sup> Macmillan Magazines Ltd 1998).

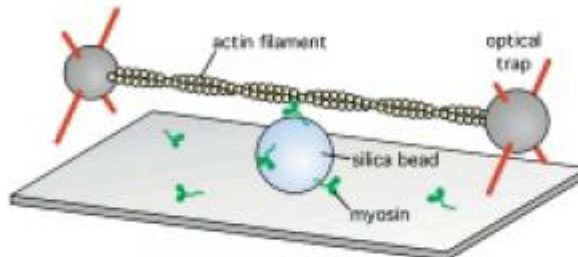
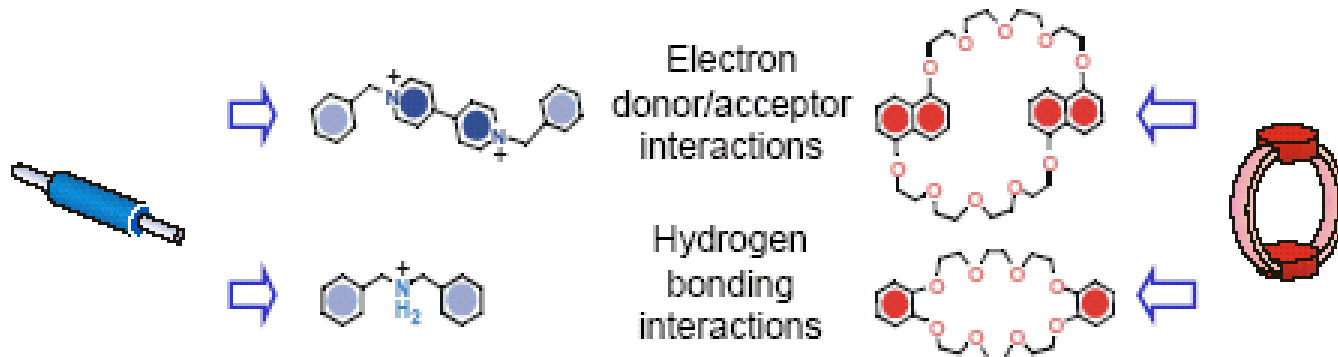
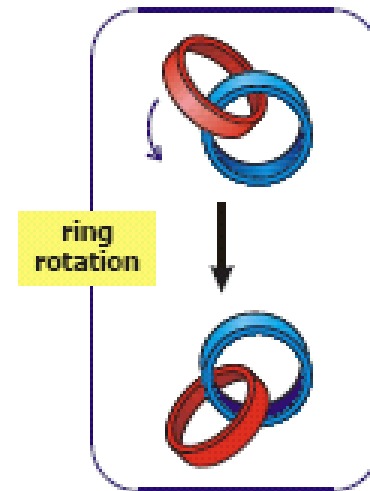
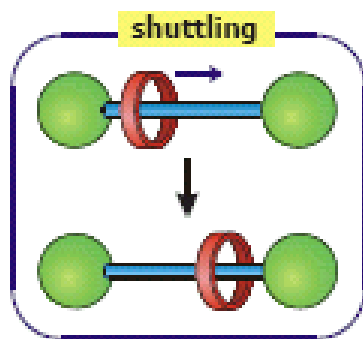
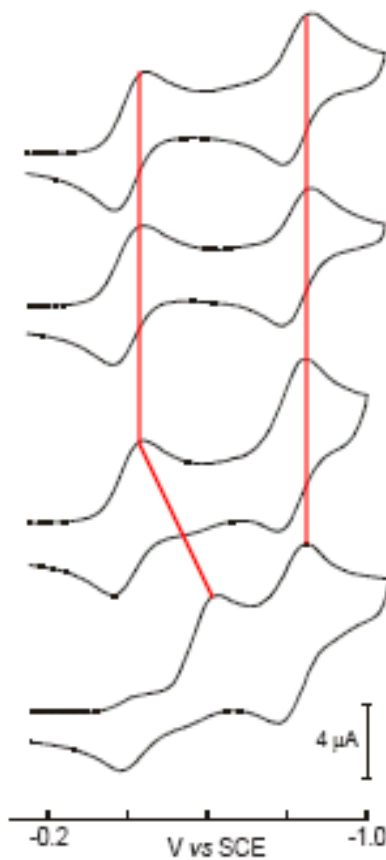
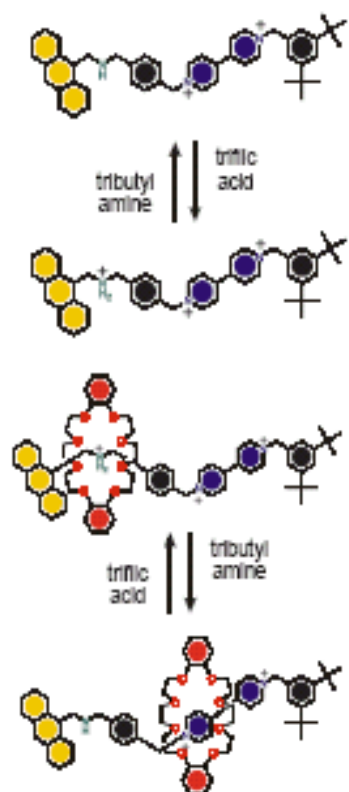
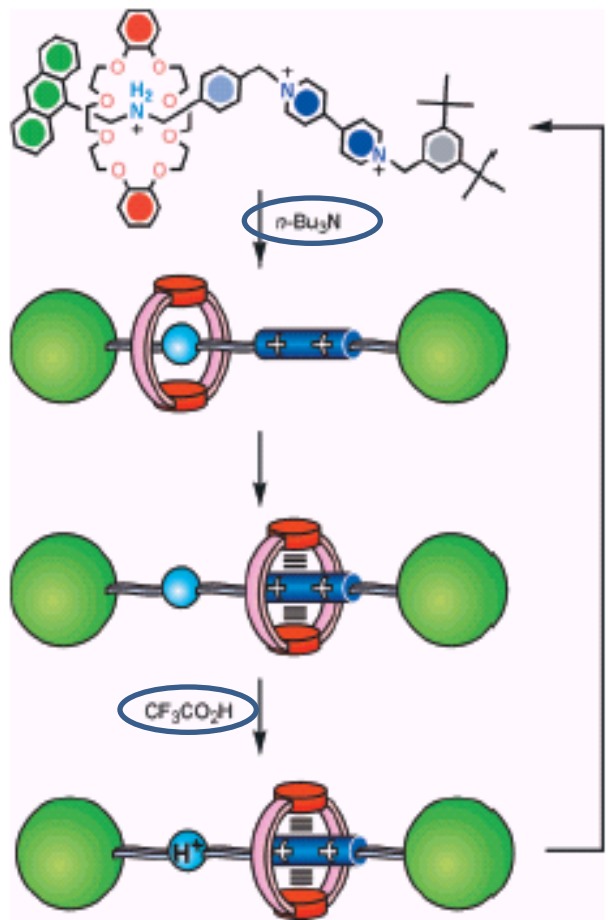
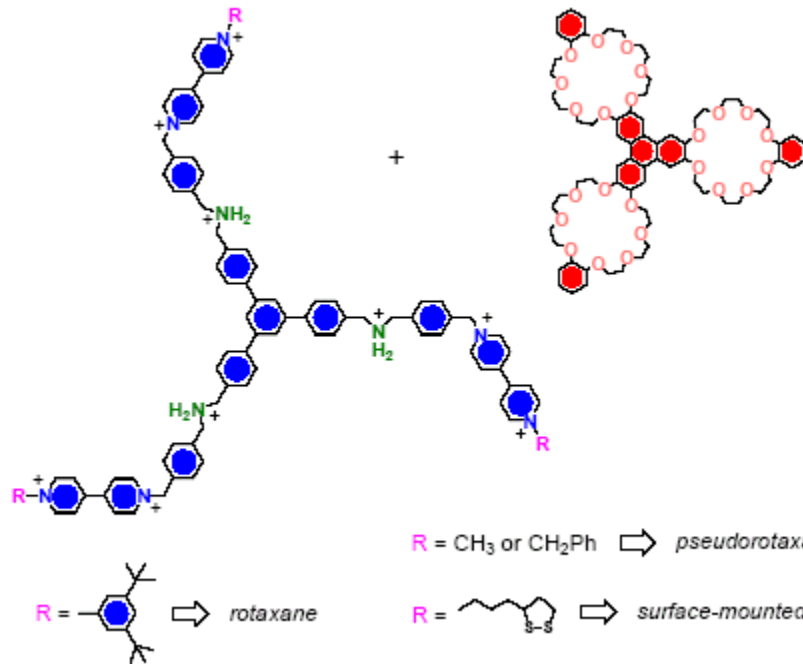


Figure 2. Experimental geometry used<sup>[19]</sup> to observe single myosin molecules binding and pulling an actin filament. The filament was attached at either end to a trapped bead. These beads were used to stretch the filament taut and move it near surface-bound silica beads that were decorated sparsely with myosin molecules. Adapted with permission from ref. [19] (Copyright<sup>®</sup> Macmillan Magazines Ltd 1994).

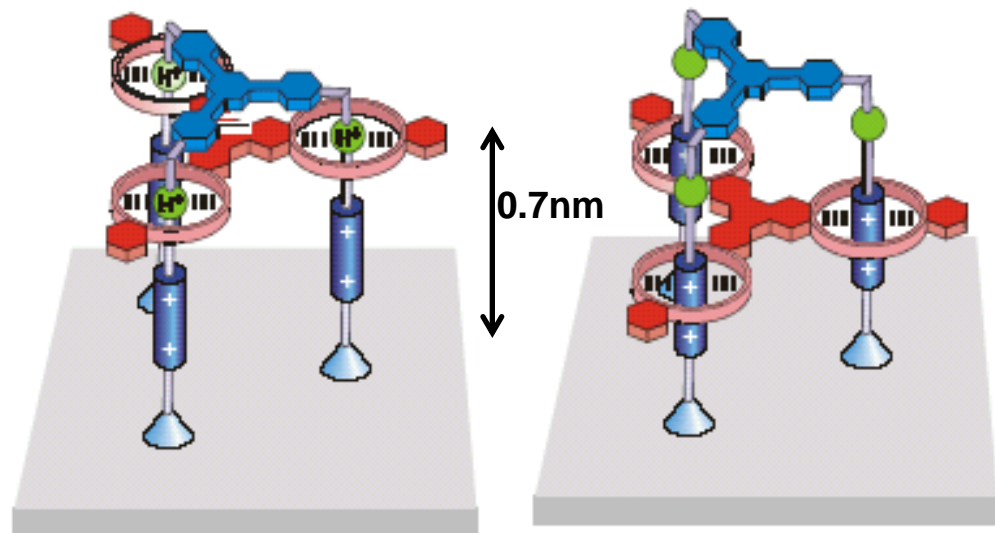
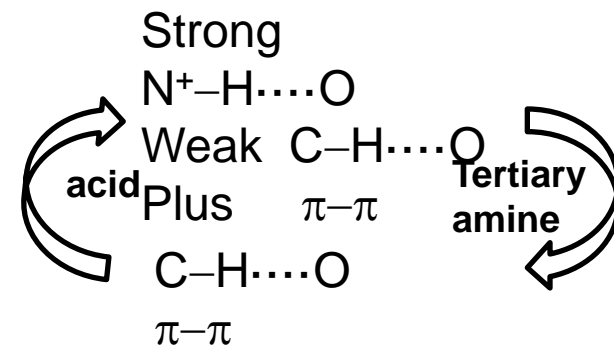


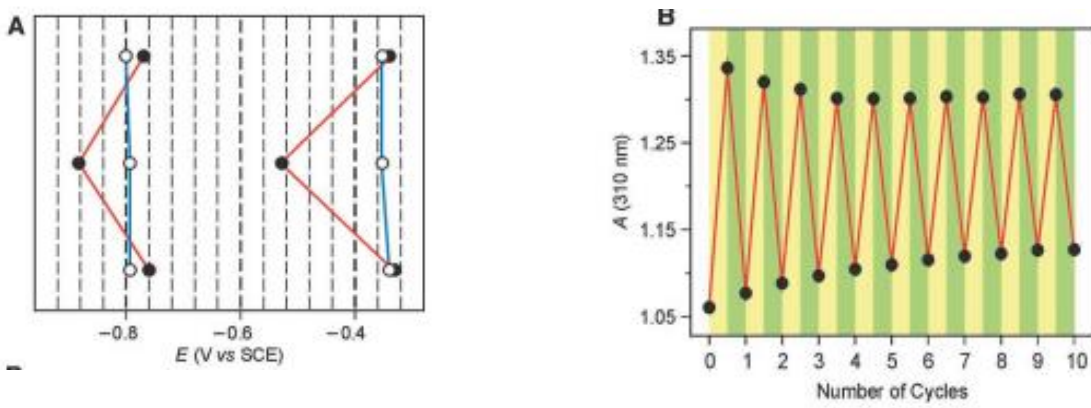
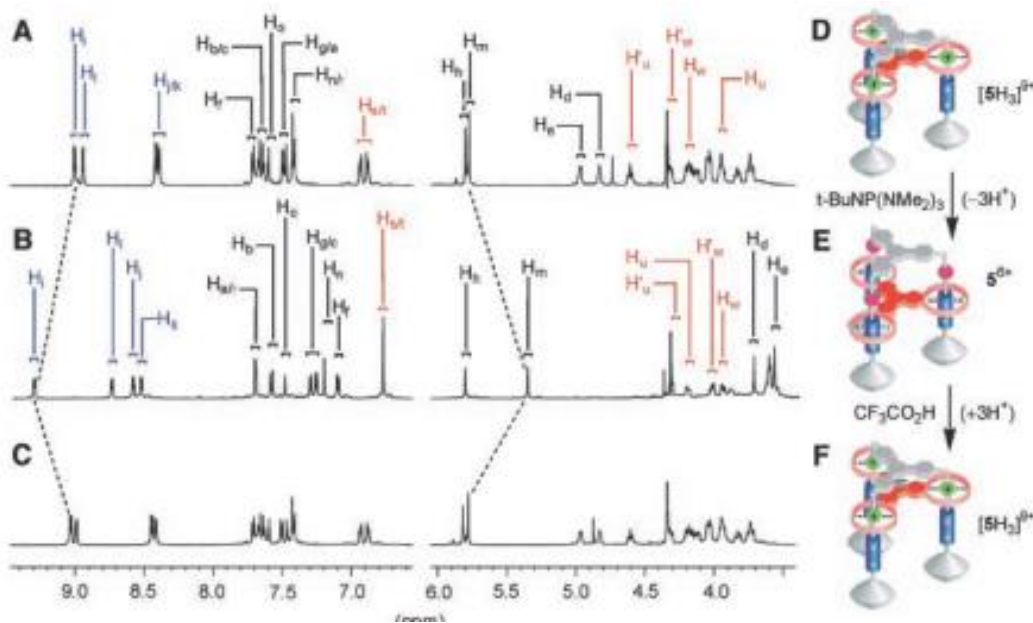
# Input chimico

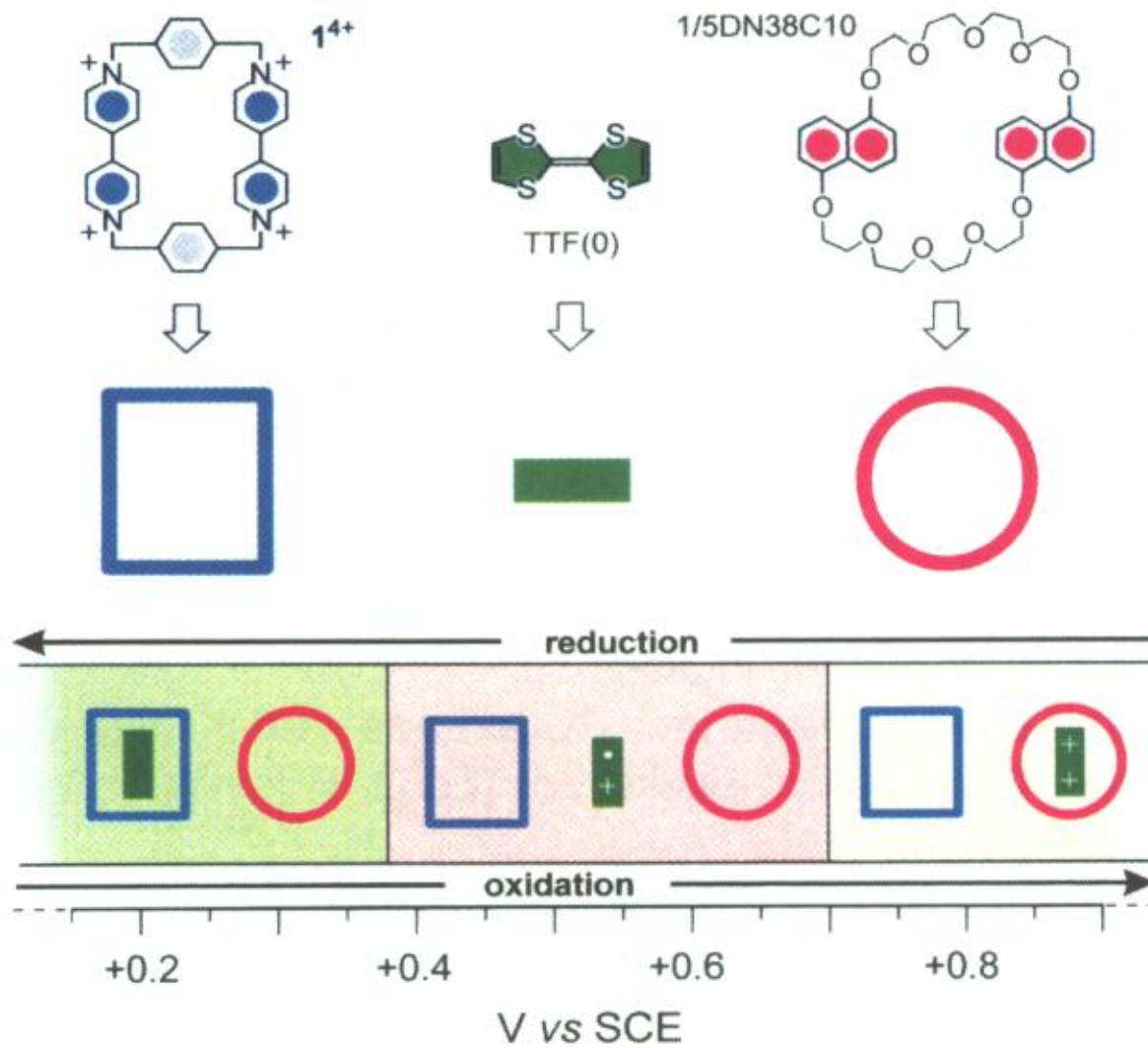




## Ascensore molecolare

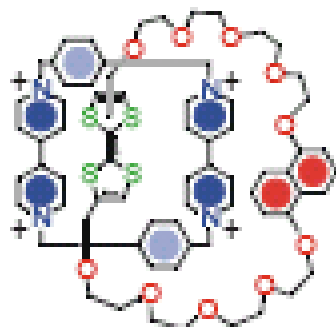




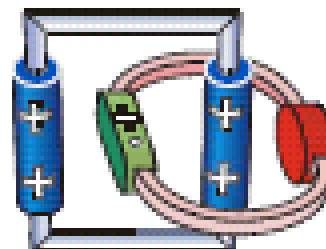


# Input elettrochimico

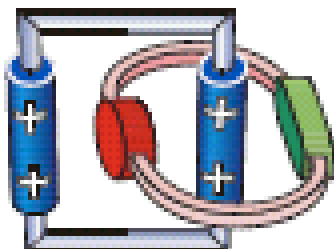
Tetratiofulvalene (0)



Tetratiofulvalene (+)



-  $e^-$   
ossidazione



+  $e^-$   
riduzione

Tetratiofulvalene (0)

Tetratiofulvalene (+)

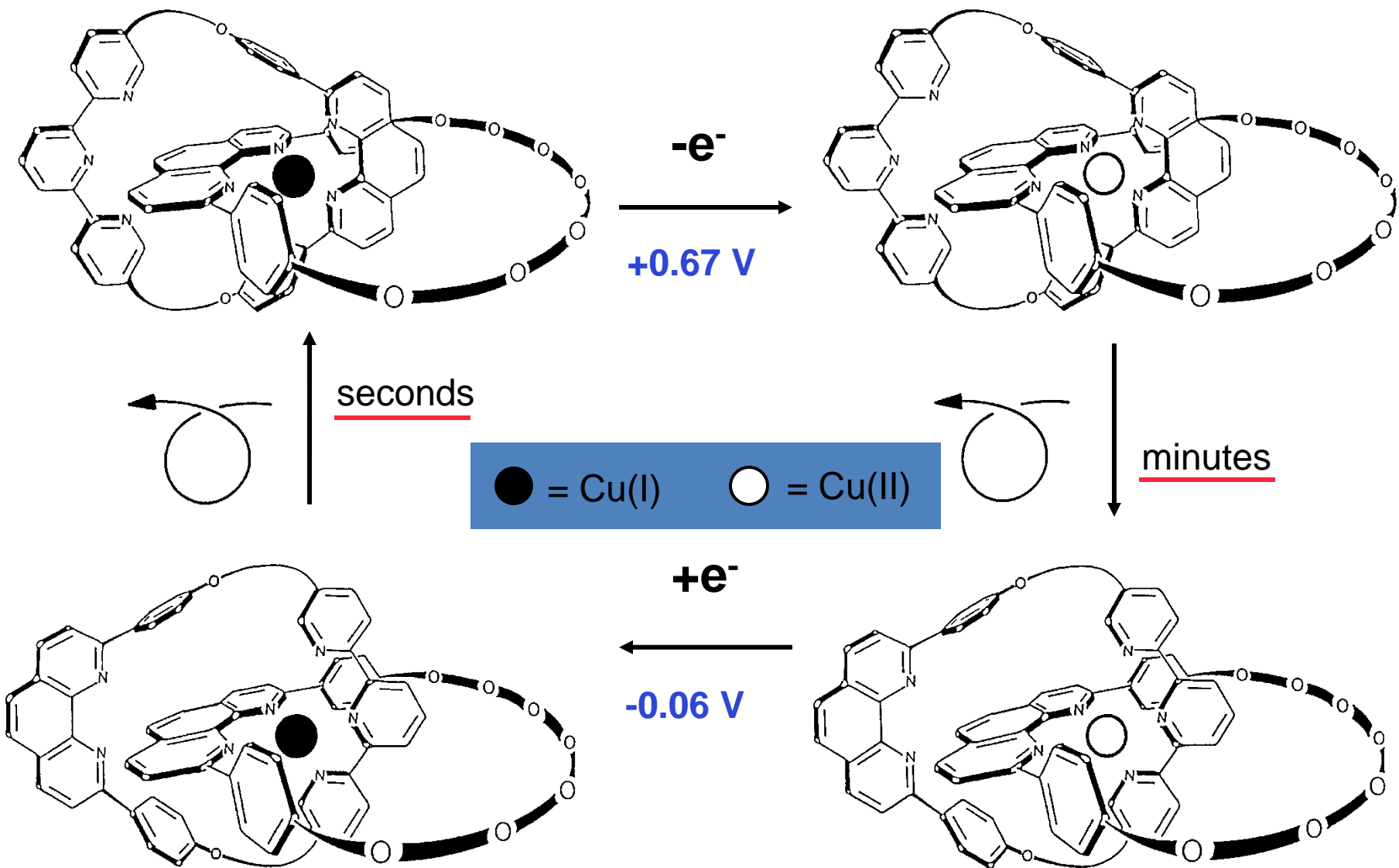
# Functionalised tetrathiafulvalene- (TTF-) macrocycles: recent trends in applied supramolecular chemistry

Chem. Soc. Rev., 2018, 47, 5614–5645

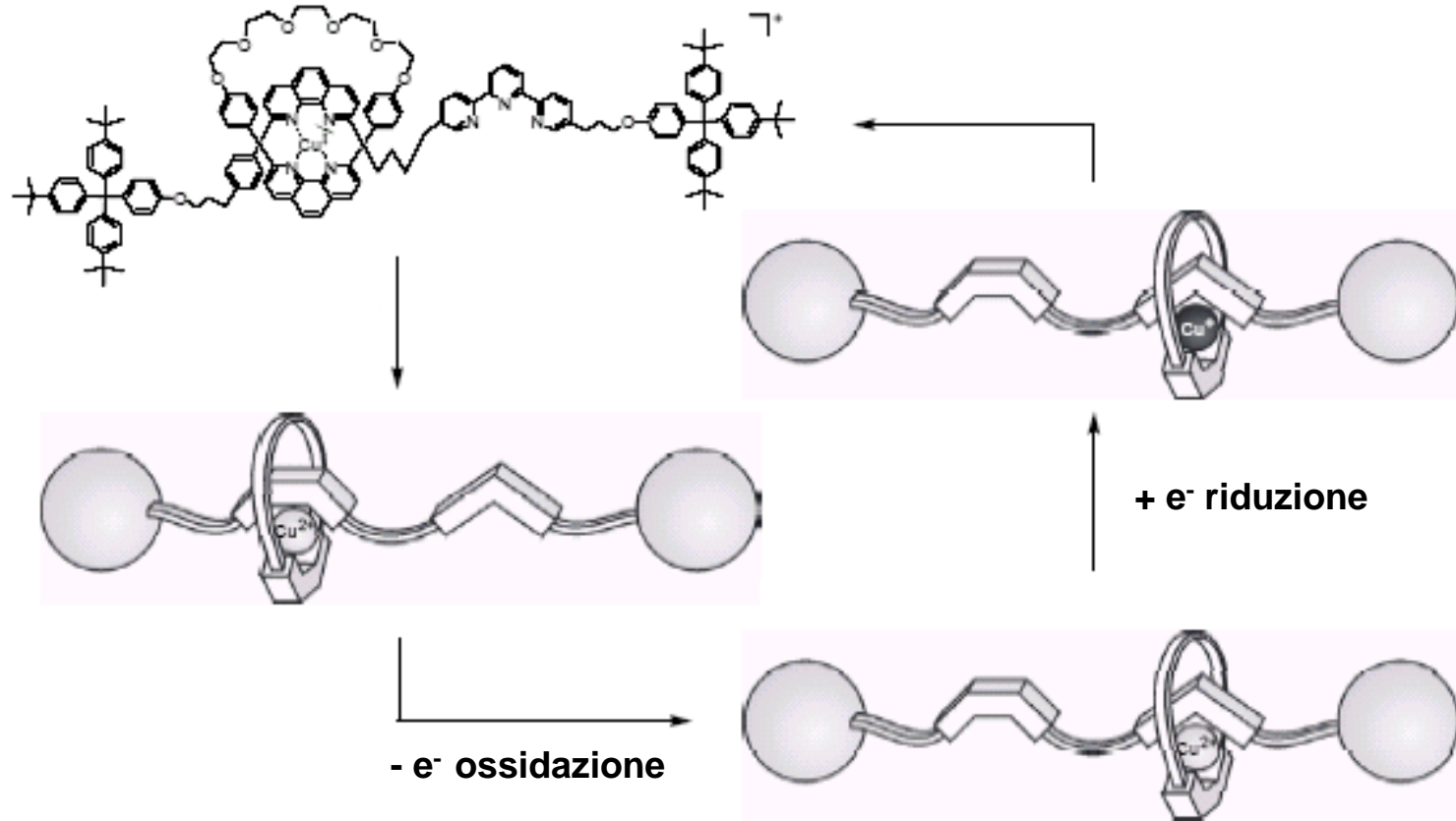
Atanu Jana, <sup>a</sup> Steffen Bähring, <sup>b</sup> Masatoshi Ishida, <sup>c</sup> Sébastien Goeb,<sup>d</sup> David Canevet, <sup>d</sup> Marc Sallé, <sup>\*d</sup> Jan O. Jeppesen <sup>\*b</sup> and Jonathan L. Sessler <sup>\*ae</sup>



# Input elettrochimico



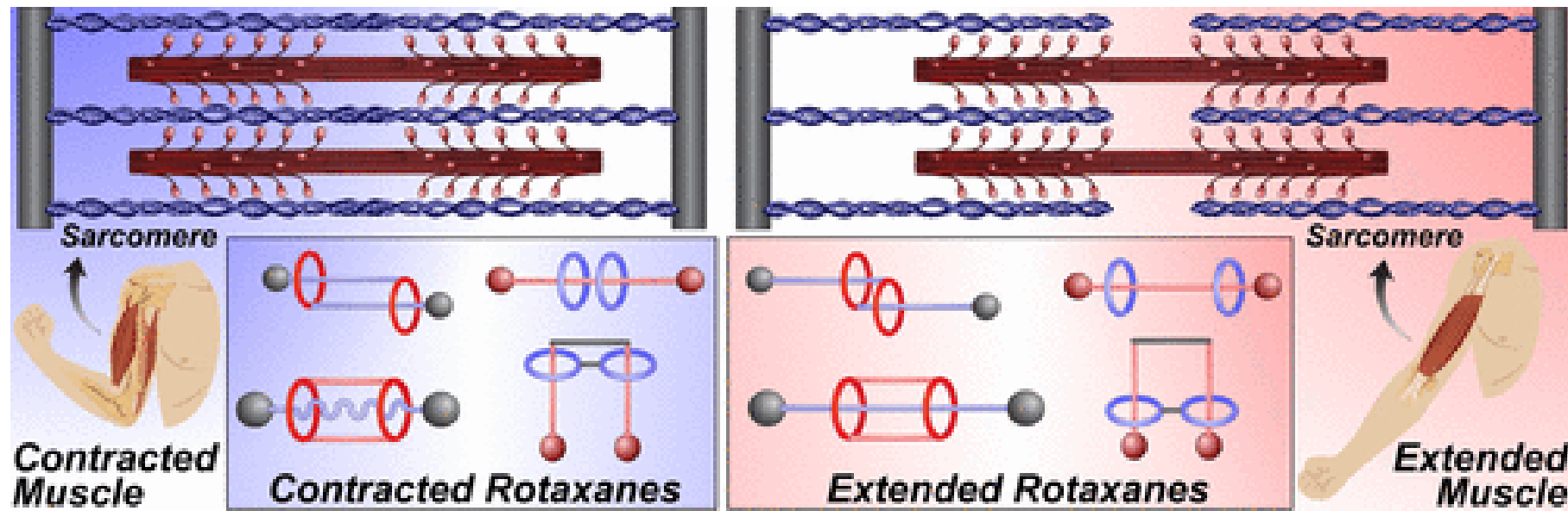
# Input elettrochimico



## Rotaxane-Based Molecular Muscles

Acc. Chem. Res. 2014, 47, 2186–2199

Carson J. Bruns and J. Fraser Stoddart\*

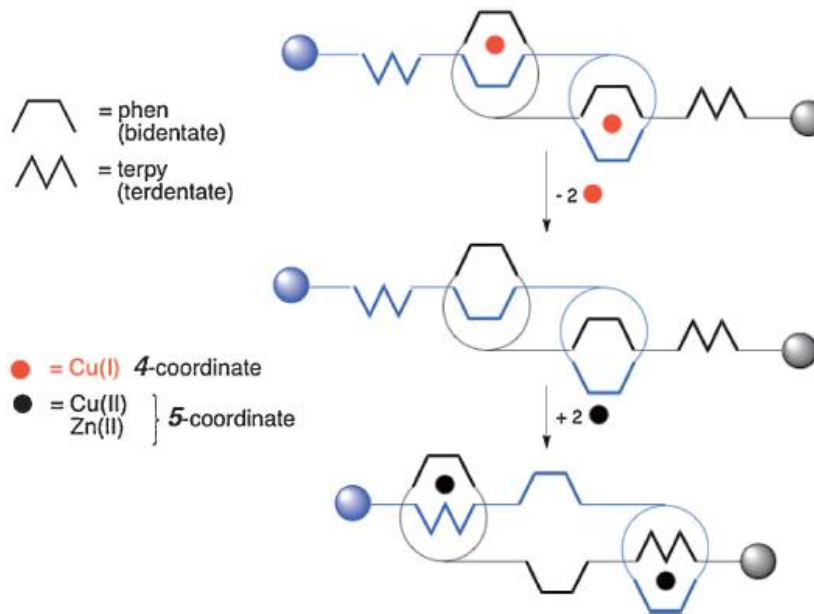


## Highlight Review

# Molecular Muscles: From Species in Solution to Materials and Devices

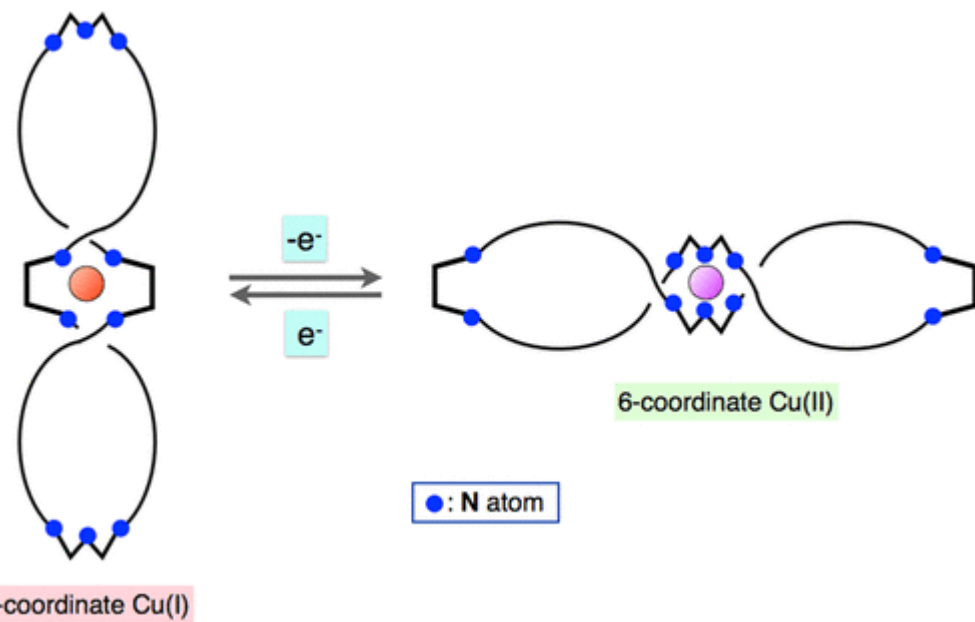
*Chem. Lett.* 2014, 43, 964–974 |

Frédéric Niess,<sup>#</sup> Vincent Duplan,<sup>#</sup> and Jean-Pierre Sauvage\*

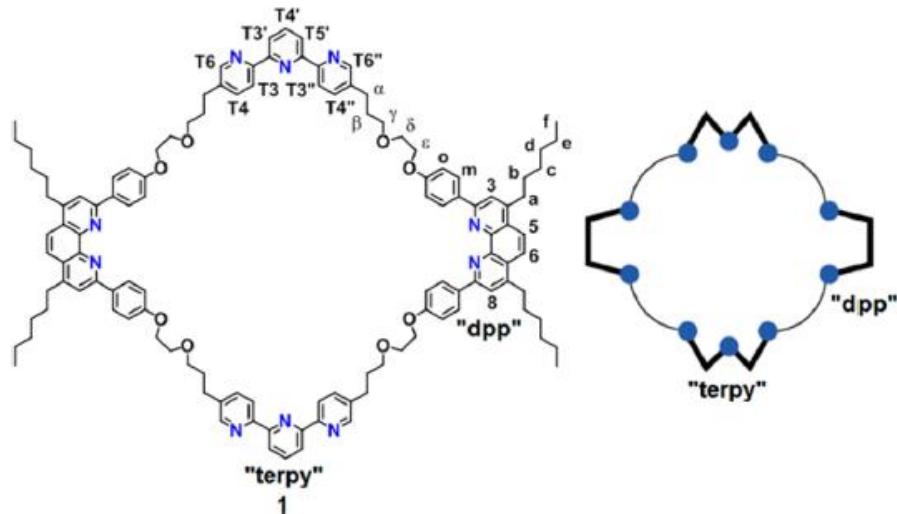


# Interconversion between a Vertically Oriented Transition Metal-Complexed Figure-of-Eight and a Horizontally Disposed One

Frédéric Niess, Vincent Duplan, and Jean-Pierre Sauvage\*



Scheme 1. Four-Coordinating-Group Macrocycle 1<sup>a</sup>



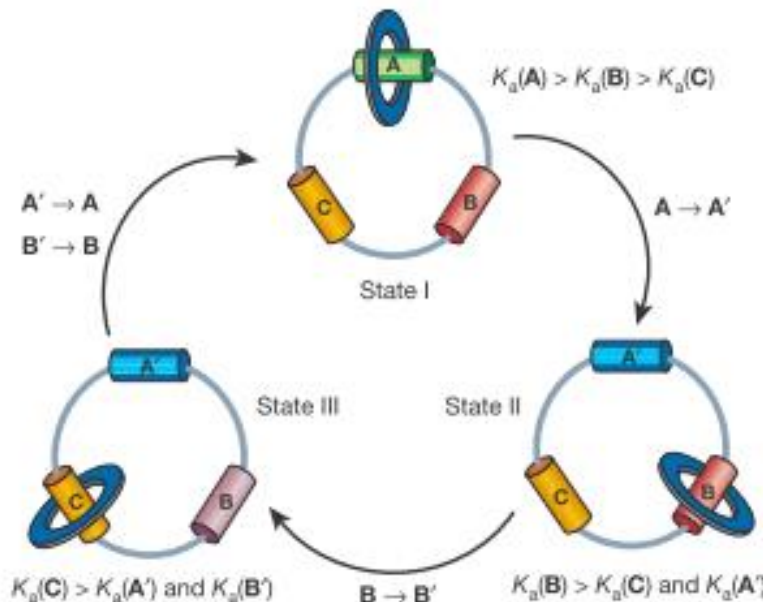
# Input fotochimico

## Unidirectional rotation in a mechanically interlocked molecular rotor

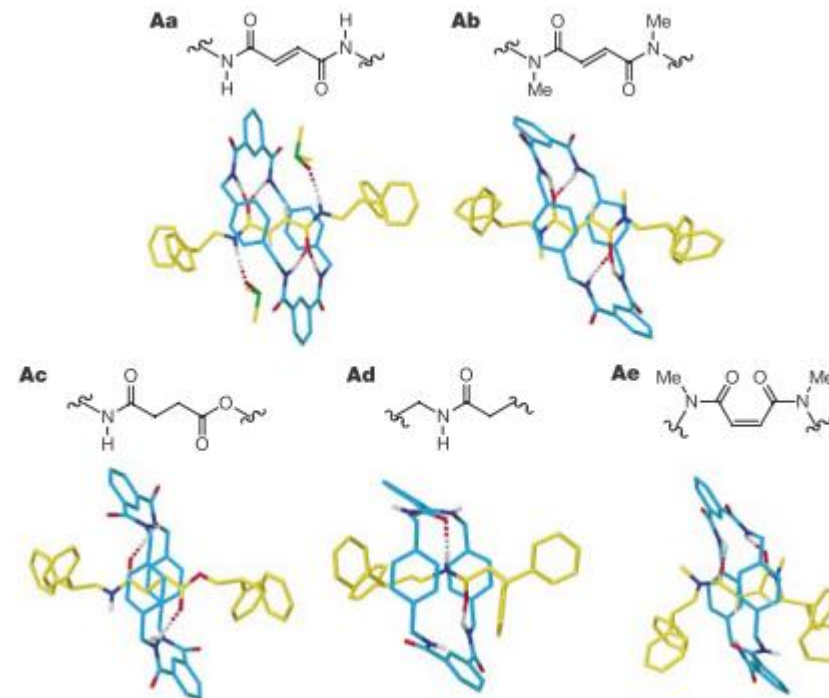
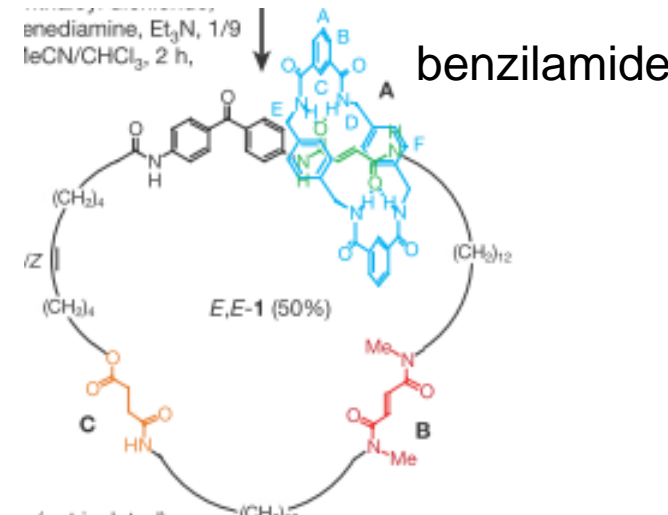
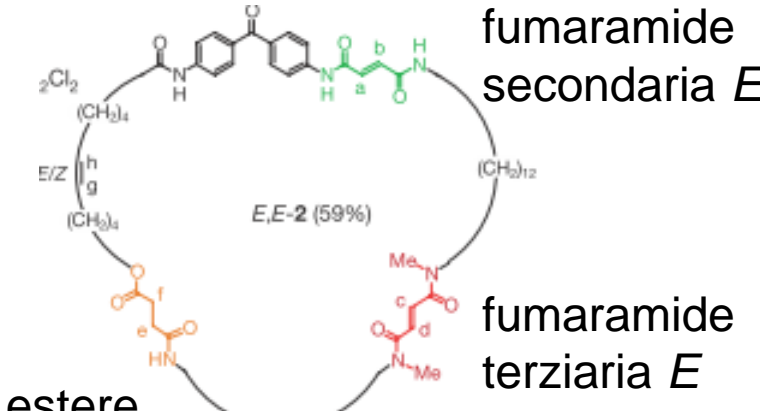
David A. Leigh\*, Jenny K. Y. Wong\*, François Dehez†  
& Francesco Zerbetto†

\* School of Chemistry, University of Edinburgh, The King's Buildings, West Mains Road, Edinburgh EH9 3JJ, UK

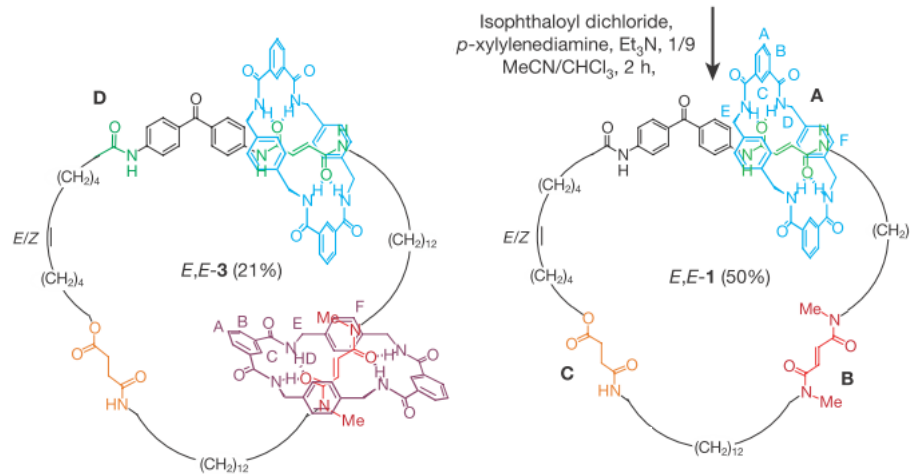
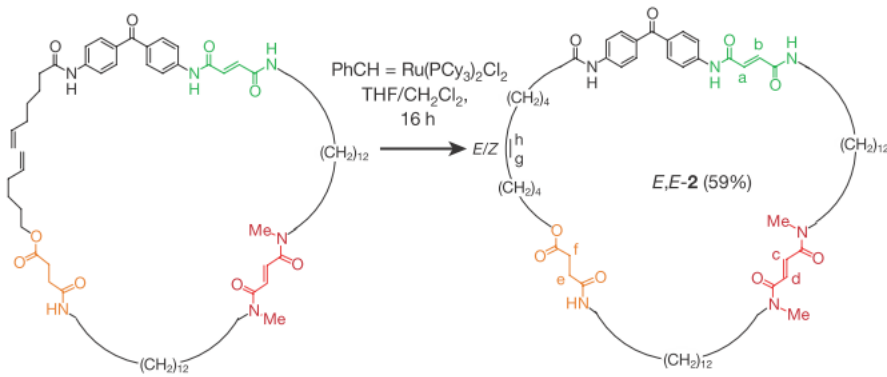
† Dipartimento di Chimica 'G. Ciamician', Università degli Studi di Bologna, via F. Selmi 2, 40126 Bologna, Italy

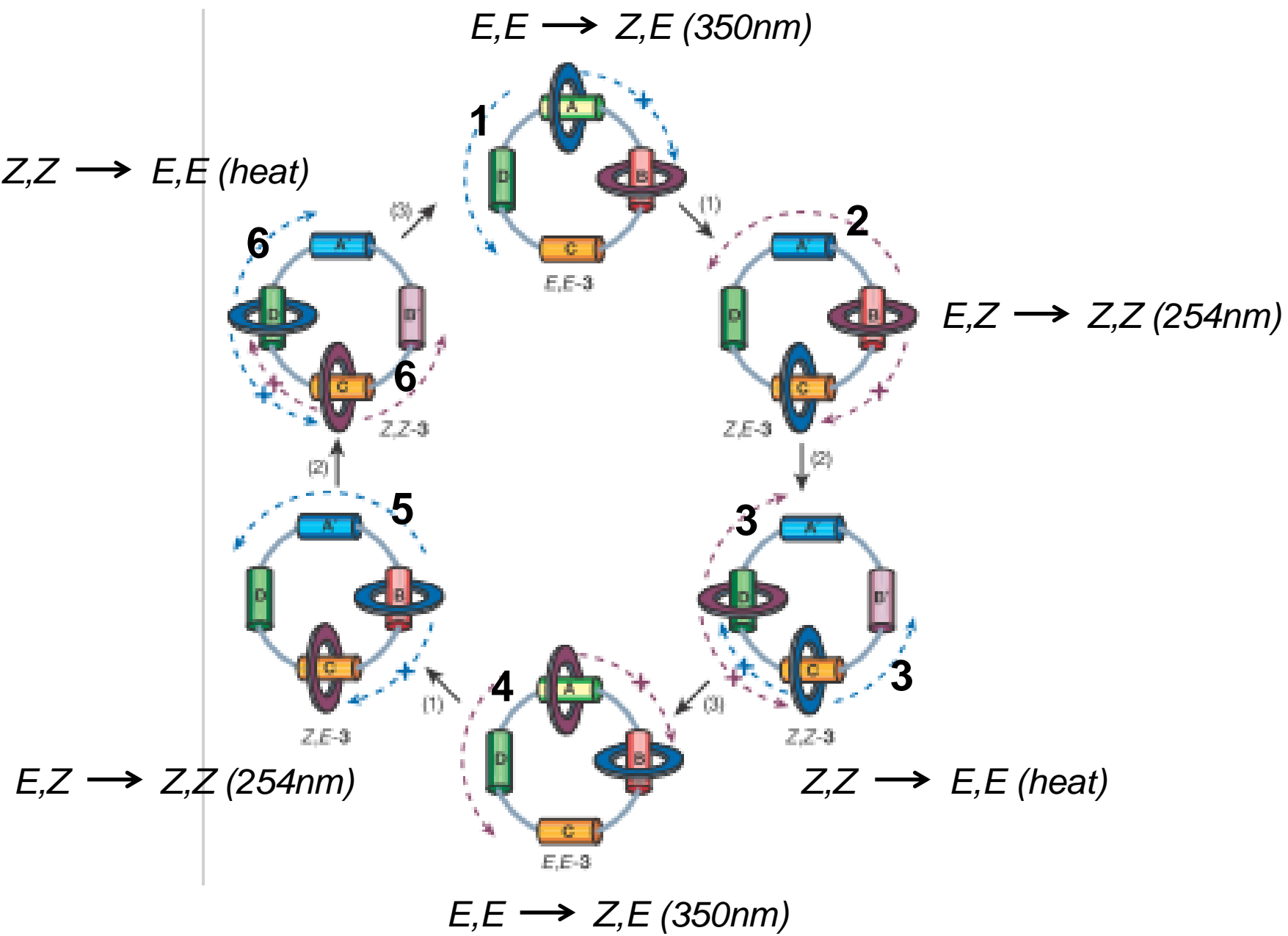


# benzofenone



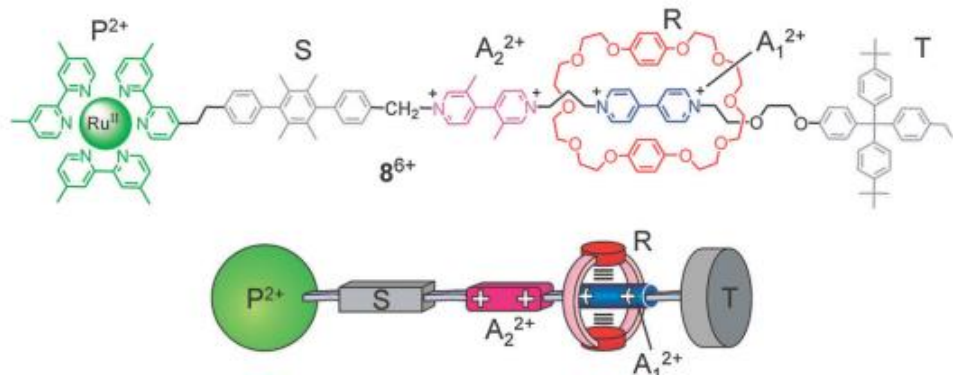
Strutture ai raggi X dei siti di binding  
dei modelli [2] rotaxani con indicati  
i legami idrogeno (in ordine di affinità)



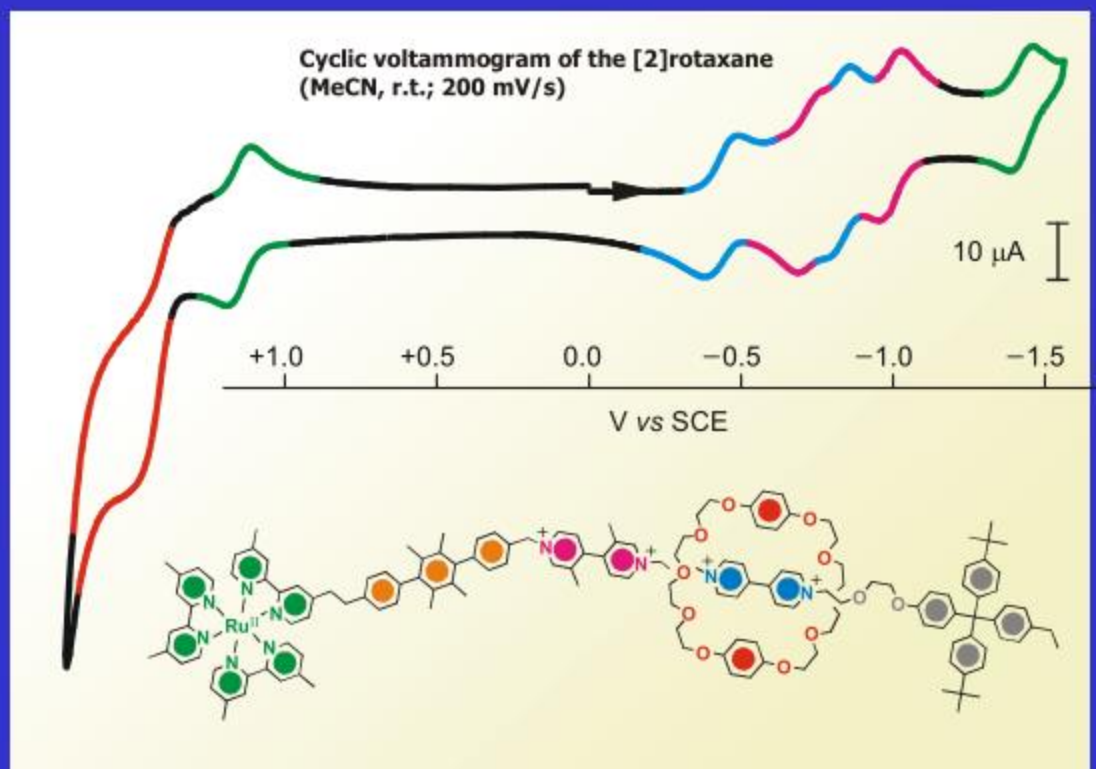
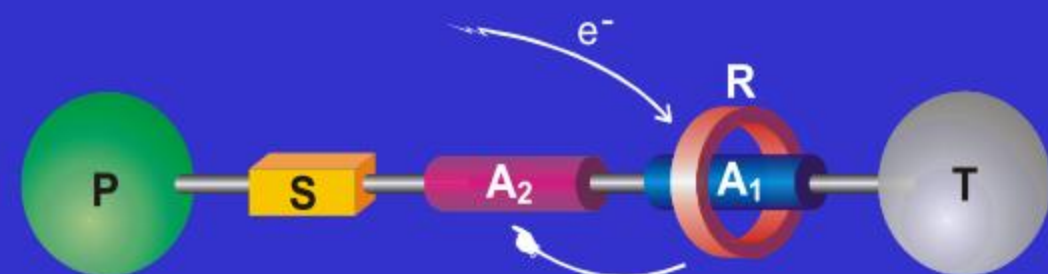


# Input fotochimico

Ru(II)polypyridine complex ( $P^{2+}$ )  
*p*-terphenyl-type rigid spacer (S)  
4,4'-bipyridinium ( $A_1^{2+}$ )  
3,3'-dimethyl-4,4'-bipyridinium ( $A_2^{2+}$ )  
Tetraarylmethane group (T)  
Six  $\text{PF}_6^-$  counterions

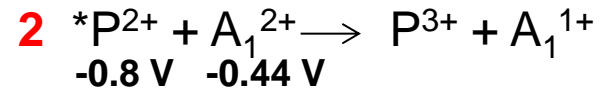
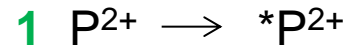
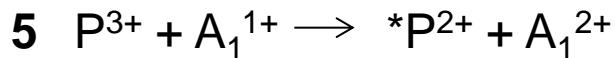
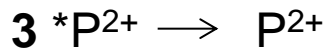
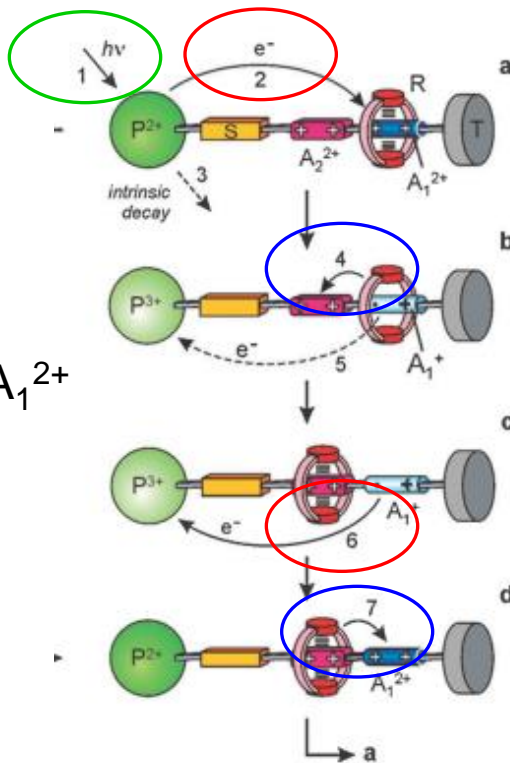
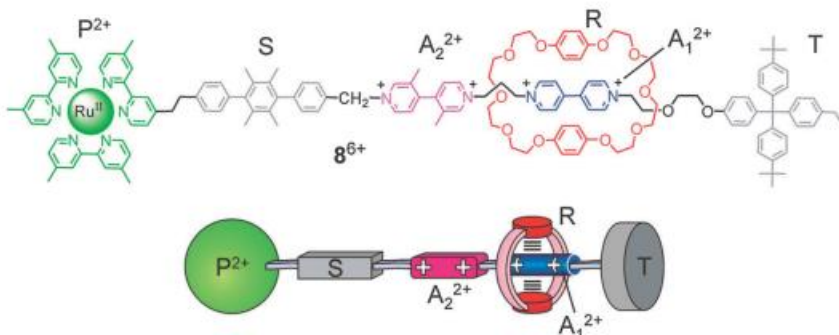


## a) Redox-induced ring motion

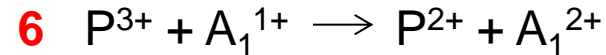


# Input fotochimico

Ru(II)polypyridine complex ( $P^{2+}$ )  
 $p$ -terphenyl-type rigid spacer (S)  
 4,4'-bipyridinium ( $A_1^{2+}$ )  
 3,3'-dimethyl-4,4'-bipyridinium ( $A_2^{2+}$ )  
 Tetraarylmethane group (T)  
 Six  $\text{PF}_6^-$  counterions

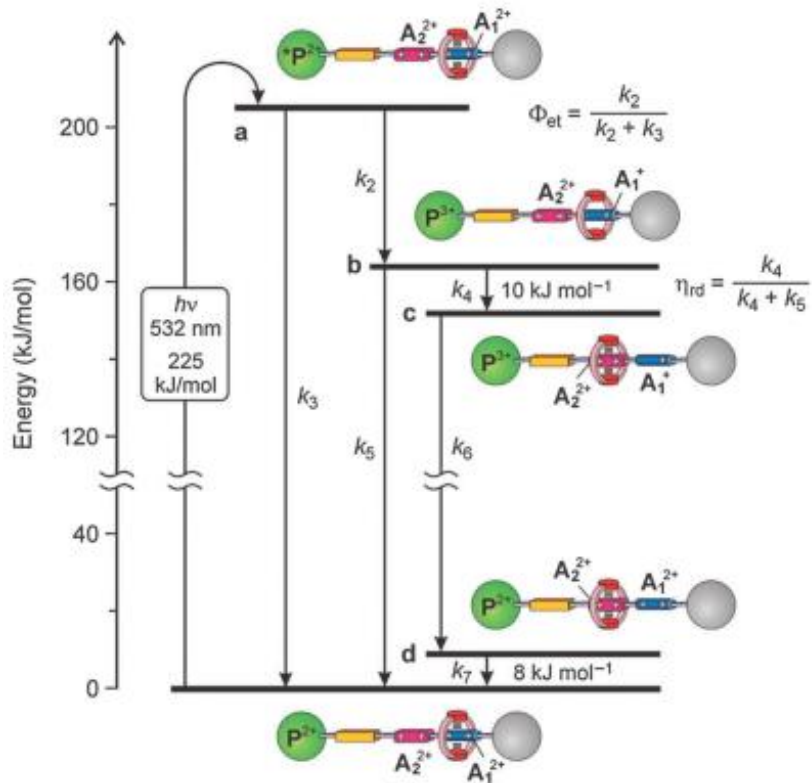


**4** Shuttling (5 nm)



**7** Shuttling (5 nm)

# Input fotochimico



Hence, the fraction  $F$  of the excited state energy ( $205 \text{ kJ mol}^{-1}$ ) used for the motion of the ring amounts to *ca.* 10%, and the overall efficiency of the machine is  $\eta = \Phi_{\text{sh}} \times F = 0.2\%$ .

This somewhat disappointing result is compensated by the fact that the investigated system gathers together the following features: (i) it is powered by visible light (in other words, sunlight); (ii) it exhibits autonomous behaviour (*i.e.*, like natural molecular motors, it operates automatically in a constant environment as long as the energy source is available); (iii) it does not generate waste products; (iv) its operation can rely only on intramolecular processes, allowing in principle operation at the single-molecule level; (v) it can be driven at a frequency of about 1 kHz; (vi) it works in mild environmental conditions (*i.e.*, fluid solution at ambient temperature); and (vii) it is stable for at least  $10^3$  cycles.

# Input fotochimico e chimico (agenti sacrificali TEA e O<sub>2</sub>)

